doi:10.1093/brain/awt275 Brain 2013: 136; 3709–3726 | 3709

BRAIN
A JOURNAL OF NEUROLOGY

Neural network connectivity differences in children who stutter

Soo-Eun Chang[1,2] and David C. Zhu[2,3,4]

1 Department of Communicative Sciences and Disorders, Michigan State University, East Lansing, MI, USA
2 Cognitive Imaging Research Centre, Michigan State University, East Lansing, MI, USA
3 Department of Psychology, Michigan State University, East Lansing, MI, USA
4 Department of Radiology, Michigan State University, East Lansing, MI, USA

Correspondence to: Soo-Eun Chang, Ph.D.,
Rachel Upjohn Building, Rm 2731,
Department of Psychiatry,
University of Michigan,
4250 Plymouth Rd.
Ann Arbor, MI 48109
E-mail: sooeunc@med.umich.edu

Affecting 1% of the general population, stuttering impairs the normally effortless process of speech production, which requires precise coordination of sequential movement occurring among the articulatory, respiratory, and resonance systems, all within millisecond time scales. Those afflicted experience frequent disfluencies during ongoing speech, often leading to negative psychosocial consequences. The aetiology of stuttering remains unclear; compared to other neurodevelopmental disorders, few studies to date have examined the neural bases of childhood stuttering. Here we report, for the first time, results from functional (resting state functional magnetic resonance imaging) and structural connectivity analyses (probabilistic tractography) of multimodal neuroimaging data examining neural networks in children who stutter. We examined how synchronized brain activity occurring among brain areas associated with speech production, and white matter tracts that interconnect them, differ in young children who stutter (aged 3–9 years) compared with age-matched peers. Results showed that children who stutter have attenuated connectivity in neural networks that support timing of self-paced movement control. The results suggest that auditory-motor and basal ganglia-thalamocortical networks develop differently in stuttering children, which may in turn affect speech planning and execution processes needed to achieve fluent speech motor control. These results provide important initial evidence of neurological differences in the early phases of symptom onset in children who stutter.

Keywords: stuttering; resting state functional MRI; DTI probabilistic tractography; basal ganglia thalamocortical loop; auditory motor integration

Abbreviations: BGTC = basal ganglia-thalamocortical; DTI = diffusion tensor imaging; M1 = primary motor cortex; SMA = supplementary motor area

Introduction

Stuttering is a speech disorder that affects smooth production of speech sounds. Occurring in 1% of the general population, and in ~5% of preschool-age children (Bloodstein, 1995), those afflicted with stuttering experience repetitions, prolongations, and 'blocking' of speech sounds that can severely compromise the fluent flow of speech. Decades of neuroimaging research have revealed some convergent findings that point to subtle functional (Fox *et al*., 1996; Braun *et al*., 1997; Watkins *et al*., 2008; Chang

Received April 30, 2013. Revised August 4, 2013. Accepted August 7, 2013. Advance Access publication October 16, 2013

et al., 2009) and structural (Foundas *et al*., 2001, 2003; Sommer *et al*., 2002; Jancke *et al*., 2004; Beal *et al*., 2007, 2012; Chang *et al*., 2008; Watkins *et al*., 2008) differences in cortical brain areas supporting auditory-motor integration for speech processing. Other studies examining intrinsic functional connectivity of brain activity based on functional MRI data (Lu *et al*., 2009, 2010; Xuan *et al*., 2012) and older PET studies (Wu *et al*., 1995, 1997), have shown differences involving the basal ganglia-thalamocortical (BGTC) loop. These findings corroborate some interesting phenomena associated with stuttering, such as the fact that auditory masking or manipulation (e.g. white noise, delayed auditory feedback) can induce fluent speech production even in severe stuttering cases, and that external auditory pacing signals such as metronome beats, when synchronized with speech production, can lead to the same fluency-inducing effect (Wingate *et al*., 2002; Alm, 2004).

One limitation so far in studies investigating the neural bases of stuttering has been that these almost exclusively have focused on examining adults who stutter. Because the vast majority of stuttering cases arise with symptom onset during early childhood (i.e. 2–4 years) (Yairi and Ambrose, 1992), adults who stutter likely would have developed compensatory strategies and neuroplastic changes associated with years of coping with stuttering. This makes it difficult to determine whether any differences between stuttering and control adult groups can truly be attributed to the pathophysiology of stuttering or to compensation for the core problem.

Here we present the first study to compare spontaneous brain activity correlations across the brain during rest (resting state functional MRI) and white matter connectivity [probabilistic tractography using diffusion tensor imaging (DTI)] in a relatively large sample of young children who stutter close to stuttering onset (between 3–9 years old), compared to age-matched children who do not stutter. Resting state functional MRI allows examination of temporally correlated brain activity across spatially distant regions across the brain, which has been shown to reflect structural connections in the correlated regions (Greicius *et al*., 2009), and/or a history of co-activity (Gusnard *et al*., 2001). Such 'functionally connected' regions also tend to overlap with networks supporting specific functions, such as working memory (Sala-Llonch *et al*., 2012), motor performance (Biswal *et al*., 1995), and language (Hampson *et al*., 2002), as well as 'default-mode' networks that are more active during rest than during task performance (Greicius, 2002). Probabilistic tractography based on DTI data allows examination of white matter structural connectivity, such that investigators can define a seed area of interest and calculate the connectivity distribution (reflecting the strength of fibre connection) of tracts to this seed area (Johansen-Berg and Behrens, 2006). In this study, resting state functional MRI and probabilistic tractography analyses were conducted in the same children to assess both functional and structural connectivity, respectively, to examine group differences in specific brain networks of interest.

We chose to examine two neural networks in stuttering children, based on emerging networks of interest from previous research on adults who stutter: (i) the BGTC loop, including the putamen, supplementary motor area (SMA), and primary motor cortex (M1); and (ii) the auditory-motor network including the pars opercularis (Brodmann area 44, inferior frontal cortex), and posterior superior temporal gyrus. Most neuroimaging studies to date examining stuttering speakers pointed to a possible core deficit in the left hemisphere networks (Sommer *et al*., 2002; De Nil *et al*., 2003; Lu *et al*., 2010; Chang *et al*., 2011), although heightened activity (Fox *et al*., 1996; Braun *et al*., 1997; De Nil *et al*., 2000) and structural volume/area increases (Foundas *et al*., 2001; Jancke *et al*., 2004; Cykowski *et al*., 2008) in right hemisphere regions were also common findings. The latter may have been compensatory processes, a question that may best be answered by examining children close to stuttering onset. Examining children rather than adults was also expected to provide clarification on whether more cortical or subcortical foci would be intrinsic to the pathophysiology of stuttering. Past studies reported anomalous basal ganglia activity in stuttering speakers (Wu *et al*., 1997), and normalization of basal ganglia activity after therapy (Giraud *et al*., 2008). We hypothesized that stuttering children would exhibit attenuated functional and structural connectivity compared with age-matched non-stuttering peers in both the auditory-motor network and in the basal ganglia thalamo-cortical networks, primarily in the left hemisphere.

Materials and methods

Participants

A total of 56 children between 3 to 9 years of age participated; all were right-handed, monolingual native North American English speaking, and without concomitant developmental disorders such as dyslexia, ADHD, learning delay, or other confirmed developmental or psychiatric conditions. All children underwent careful screening to ensure normal speech and language developmental history except for presence of stuttering in the stuttering group. The stuttering children and controls were matched in chronological age, and did not differ in socioeconomic status (Hollingshead, 1975). All participants were right-handed on the Edinburgh handedness inventory (Oldfield, 1971). All participants were tested on a battery of standardized speech, language, and cognitive tests, audiometric hearing screening, oral-motor screening, and cognitive evaluations. The tests included the Peabody Picture Vocabulary Test (PPVT-4), Expressive Vocabulary Test (EVT-2), Goldman-Fristoe Test of Articulation (GFTA-2), Fluharty Preschool Speech and Language Screening Test (for children <4 years of age), Test of Language Development (TOLD-P:3, I:4), Wechsler Preschool and Primary Scale of Intelligence (WPPSI-III; for children 2:6–7:3), Wechsler Abbreviated Scale of Intelligence (WASI; for children 7 and up), and the Purdue Pegboard test (Association APT, 2010). For study inclusion the participants had to score >-2 standard deviations of the norm on all standardized tests.

Stuttering severity was assessed by collecting samples of spontaneous speech, elicited through storytelling and conversational tasks with a parent and a certified speech-language pathologist. These samples were video-recorded for further offline analyses. The Stuttering Severity Instrument (SSI-4) was used to examine frequency and duration of disfluencies occurring in the speech sample, as well as any physical concomitants associated with stuttering. These were incorporated into a composite stuttering severity rating. To determine measurement reliability of the stuttering severity instrument score ratings,

an intra-class correlation coefficient was calculated on the two judges' ratings of stuttering severity instrument from each child's speech sample.

In addition to the speech-language and cognitive tests, all children were trained during a separate visit with a mock scanner to familiarize them with the scanner environment and procedures, and to practice keeping still while lying down inside the bore for stretches of time. Recordings of MRI sounds were played during this session, so that children were aware that they would be hearing loud MRI sounds during scanning. This session was repeated in some children, as needed.

All procedures used in this study were approved by the Michigan State University Institutional Review Board. All children were paid a nominal remuneration and were given small prizes (e.g. stickers) for their participation.

MRI acquisition

All MRI scans were acquired on a GE 3 T Signa® HDx MR scanner (GE Healthcare) with an 8-channel head coil. During each session, 180 T_1-weighted 1-mm^3 isotropic volumetric inversion recovery fast spoiled gradient-recalled images (10 min scan time), with CSF suppressed, were obtained to cover the whole brain with the following parameters: time of echo = 3.8 ms, time of repetition of acquisition = 8.6 ms, time of inversion = 831 ms, repetition time of inversion = 2332 ms, flip angle = 8°, field of view = 25.6 cm × 25.6 cm, matrix size = 256 × 256, slice thickness = 1 mm, and receiver bandwidth = ± 20.8 kHz.

After the T_1 data acquisition, high-order shimming procedures were carried out to improve magnetic field homogeneity. DTI data were acquired with a dual spin-echo echo-planar imaging (EPI) sequence for 12 min and 6 s with the following parameters: 48 contiguous 2.4-mm axial slices in an interleaved order, field of view = 22 cm × 22 cm, matrix size = 128 × 128, number of excitations (NEX) = 2, echo time = 77.5 ms, repetition time = 13.7 s, 25 diffusion-weighted volumes (one per gradient direction) with b = 1000 s/mm^2, one volume with b = 0 and parallel imaging acceleration factor = 2.

To study rest state brain function, echo-planar images, starting from the most inferior regions of the brain, were acquired for 7 min with the following parameters: 38 contiguous 3-mm axial slices in an interleaved order, echo time = 27.7 ms, repetition time = 2500 ms, flip angle = 80°, field of view = 22 cm, matrix size = 64 × 64, ramp sampling, and with the first four data points discarded. Each volume of slices was acquired 164 times while a subject was asked to relax and keep his/her eyes closed, but encouraged not to fall asleep.

One staff member sat inside the scanner room next to the child at all times to monitor the child's comfort and to ensure cooperation during scanning. During acquisition of MPRAGE and DTI scans, the children viewed a children's movie, which was turned off before the start of the resting state scans.

Structural MRI data preprocessing and functional-structural data alignment

The structural MRI data was processed using Freesurfer version 5.0 (http://surfer.nmr.mgh.harvard.edu/). Freesurfer comprises a package of automated algorithms that allow calculation of surface mesh representations of the cortex based on individual participants' T_1-weighted volumetric images. Detailed steps involved have been described elsewhere (Yeo *et al*., 2011). Briefly, each subject's T_1-weighted magnetic resonance volumetric images were preprocessed through the default FreeSurfer steps, which included the following: motion correction, skull stripping, non-linear registration (warping) from the original space to the MNI305 space (standard space), cortical and subcortical segmentations, regional volume and cortical thickness measurements, spherical mapping and registration, and cortical parcellation.

A notable strength of using the preprocessing steps offered by Freesurfer is that it allows surface-based registration of participants' structural data, which significantly improves alignment of cortical landmarks compared to volume-based registration. Another strength that is especially relevant when preprocessing paediatric MRI data is that surface-based registrations have been shown to lead to significantly less registration error, and when tested with children's brains down to 4 years of age it was shown that registration to a common space did not result in age-associated bias (Ghosh *et al*., 2010). We visually confirmed the accuracy of registering each child's T_1-weighted magnetic resonance volumetric image to standard space. For each subject, a transformation matrix was created by FreeSurfer during warping steps, which was used to register each child's functional and structural connectivity maps to the MNI 305 standard space. All whole-brain group analyses were carried out in the standard space. Anatomical regions segmented with FreeSurfer were applied to all region of interest-based connectivity analyses described below.

Generation of seed regions for connectivity analyses

To define seed regions in the BGTC and auditory-motor networks for the purpose of functional connectivity analyses, we first grossly defined the relevant anatomical regions based on automatically generated parcellation maps from FreeSurfer (Fischl *et al*., 2002). The grey matter maps were limited to the grey matter mantle and did not include white matter. Each region of interest was shape preserved, and followed the anatomy of each individual's gyral and sulcal structure of the specific area. We then manually edited each of these seed regions in each subject by limiting the volume to within a 15 mm sphere from the centre of mass of each seed region. This ensured that there was relative consistency across participants in the size of the regions of interest. Examples of the edited seed areas are shown in Supplementary Fig. 1. The seed regions included the pars opercularis [Brodmann area (BA) 44], SMA, putamen, posterior superior temporal gyrus (manually edited to only include the area posterior to the first Heschl's sulcus). For each of these regions, the white matter regions immediately subjacent to the grey matter area were used as seed regions for DTI fibre tracking. These white matter regions were defined using FreeSurfer to include white matter tissue within 5 mm of the grey/white matter boundary. This approach allows for integrated understanding of the functional and structural connectivity from a common anatomical region and has been successfully applied to research in Alzheimer's disease (Zhu *et al*., 2013).

Resting-state fMRI individual-subject data processing

Resting state functional MRI correlation analysis was conducted using AFNI (Cox, 1996), in each subject's original space. For each subject, the acquisition timing difference was first corrected for different slice locations. With the last functional volume as the reference, rigid-body motion correction was done in three translational and three rotational directions. The amount of motion was estimated and then modelled in data analysis. For each subject, spatial blurring with a full-width half-maximum of 4 mm was used to reduce random noise and inter-subject anatomical variation during group analysis. At each voxel, motion

estimation parameters, baseline, linear and quadratic system-induced signal trends were removed from the time courses using the '3dDeconvolve' routine in AFNI. Brain global, CSF and white matter mean signals were modelled as nuisance variables and removed from the time courses. In order to create the time course from pure CSF regions, the lateral and third ventricles on the high-resolution T_1-weighted volumetric images were segmented using FreeSurfer software followed by 1 mm^3 erosion. For the same reason, the white matter was segmented from the T_1-weighted volumetric images using the 'FAST' routine in the FSL software (Smith *et al*., 2004) followed by 4 mm × 4 mm × 4 mm cubical erosion. The cleaned time courses were then bandpass filtered in the range of 0.009–0.08 Hz (Fox *et al*., 2005). These filtered time courses were used for correlation-based connectivity analyses. The '3dfim+' routine in AFNI was used to correlate the time course in every voxel of the brain against the space-averaged time course from a seed region.

Resting-state fMRI between-group statistical comparisons

To prepare for group analysis, the correlation coefficients were converted to Z values through Fisher's Z-transformation. After warping to the MNI305 standard space, the data were spatially blurred with full-width half-maximum of 2 mm to reduce potential noise generated by non-linear warping. Between-group *t*-tests were performed on these Z values. Monte Carlo simulation was performed according to the matrix and voxel size of the imaging volume, and voxel intensity thresholding, masking and spatial blurring applied. Cluster identification was used to estimate overall statistical significance with respect to the whole brain (Ward, 2000). The between-group *t*-test results for functional connectivity with a seed were corrected for multiple comparisons based on the following criteria: a voxel was considered significant only if it was within a 425 mm^3 cluster in which the voxels were connected and all had a voxel-based $P \leqslant 5 \times 10^{-3}$. Based on the application of these criteria to the whole brain, the voxel-based $P \leqslant 5 \times 10^{-3}$ was corrected to be an equivalent whole-brain $P \leqslant 0.032$.

Region of interest-based functional connectivity analyses

In addition to seed-based whole brain comparisons of functional connectivity between groups, we also examined group differences in the correlations between *a priori* defined pairs of seed regions (LBA44-LpSTG, LBA44-LM1, RBA44-RpSTG, RBA44-RM1 for the auditory-motor network; LPutamen-LSMA, LSMA-LM1, LPutamen-LM1, LPutamen-LpSTG, for the BGTC network). For these analyses, we first extracted the cleaned and filtered time courses from each pair of seed regions for each subject as described above. Pearson correlation coefficients were calculated between each pair of time courses at the corresponding seed regions. These coefficients were then converted to Z values through Fisher's Z-transformation. Mixed-effects ANOVAs with group and sex as between-group variables and subject as a random variable, were used to compare the Z values between groups. As it was expected that age might have an influence on inter-regional correlations, age (in months) was entered as a covariate. Because of group differences in verbal IQ, we also added this variable as a covariate of no interest. Results were considered significant given a $P < 0.05$. Bonferroni correction was applied to control for false positive findings due to the multiple comparisons.

Diffusion tensor imaging fibre tracking and between-group statistical comparison

Probabilistic fibre tracking was performed using routines from the FSL Diffusion Toolbox (FDT v2.0) (http://fsl.fmrib.ox.ac.uk/fsl/fsl-4.1.9/fdt/fdt_probtrackx.html). After eddy-current distortion and motion correction, Bayesian Estimation of Diffusion Parameters Obtained using Sampling Techniques with crossing fibres modelled ($n = 2$) (BEDPOSTX) (Behrens *et al*., 2007) was performed at each voxel. Then, probabilistic tractography with the 'PROBTRACKX' routine was applied to calculate whole brain connectivity distributions from each subject-specific seed region. The connectivity distribution maps were then warped to the MNI305 standard space. The data were spatially blurred with full-width half-maximum of 2 mm to reduce the noise due to non-linear warping. Between-group *t*-tests were performed. Monte Carlo simulation was performed according to the matrix and voxel size of the imaging volume, voxel intensity thresholding, masking and spatial blurring applied. Based on the result of Monte Carlo simulation, a voxel was considered significant only if it was within a 30.8 mm^3 cluster in which the voxels were connected and all had a voxel-based $P \leqslant 5 \times 10^{-3}$. Based on the application of these criteria to the whole brain, a voxel-based $P \leqslant 5 \times 10^{-3}$ was corrected to an equivalent whole-brain $P \leqslant 0.033$.

Results

Behavioural assessments

The stuttering and control groups' demographic data and results of standardized testing are shown in Table 1. As shown here, the children from the two groups did not differ on any of the standardized speech-language measures administered nor on measures of socioeconomic status, manual dexterity, or handedness. With the exception of two children in the stuttering group who scored below one standard deviation (SD) on the Goldman-Fristoe Test of articulation, none of the children scored <1 SD on any of the speech-language measures. Children in the two groups did not differ significantly in any of these standardized assessments (Table 1). The two groups did not differ on the performance IQ, but differed on verbal IQ scores. Hence, verbal IQ scores were entered as a covariate in our statistical analyses of group differences in the brain data.

For children who stutter, average time since stuttering onset (duration of stuttering) was 38.8 months (SD = 26.4) and stuttering onset age according to parent report was at an average of 36.2 months (SD = 11.2), which is consistent with previously reported typical onset age for stuttering (Yairi and Ambrose, 1992). Children who stutter had an average stuttering severity instrument score of 20.48 (SD = 7.11) corresponding to a 'moderate' stuttering severity. The stuttering severity among the participants ranged from very mild to very severe. The intra-class correlation coefficient for the overall stuttering severity instrument measurement between two independent judges was 0.98. Per cent stuttered disfluencies (e.g. sound-syllable repetitions, word repetitions, audible and inaudible sound prolongations), and normal disfluencies (e.g. interjections, phrase repetitions, revisions, etc.), were also

Table 1 Participant demographic information and behavioural test results

Measures	Stuttering	Controls	Difference
n	27	29	n/a
Age in months	77.1 (26.7)	76.9 (22.8)	$P = 0.979$ (n.s.)
SSI-4	20.5 (7.1)	N/A	n/a
% stuttered disfl	5.7 (4.5)	0.97 (.82)	$P = 0$ (significant)
% normal disfl	5.0 (3.0)	4.3 (2.2)	$P = 0.782$ (n.s.)
PPVT-IV	109.5 (14.3)	116.4 (14.9)	$P = 1$ (n.s.)
EVT	106.5 (13.3)	114.5 (16.1)	$P = 0.653$ (n.s.)
GFTA	103.8 (9.2)	105.0 (8.9)	$P = 0.606$ (n.s.)
Handedness	74.9 (27.8)	83.9 (15.7)	$P = 0.146$ (n.s.)
Full IQ	102.5 (15.8)	113.9 (15.8)	$P = 0.135$ (n.s.)
Verbal IQ	102.3 (15.5)	117.3 (16.7)	$P = 0.017$ (significant)
Performance IQ	105.3 (14.9)	112.6 (19.1)	$P = 1$ (n.s.)
Purdue[a]: dominant hand	9.30 (2.88)	9.10 (2.74)	$P = 1$ (n.s.)
Purdue: non-dominant hand	8.44 (2.90)	8.38 (2.81)	$P = 1$ (n.s.)
Purdue: both hands	6.70 (2.97)	7.05 (2.81)	$P = 1$ (n.s.)
SES	52.6 (8.2)	53.1 (7.6)	$P = 0.817$ (n.s.)

[a]Number of pegs completed in 30 s.
SSI-4 = Stuttering Severity Instrument, fourth edition; % stuttered disfl = stuttered words (e.g. sound-syllable repetitions, word repetitions, sound prolongations) occurring per 100 words during conversational speech; % normal disfl = normal disfluencies (e.g. interjections, phrase repetitions) occurring per 100 words during conversational speech; PPVT = Peabody Picture Vocabulary Test; EVT = Expressive Vocabulary Test; GFTA = Goldman-Fristoe Test of Articulation; Purdue = Purdue pegboard test; SES = Hollingshead four-factor index of social status; n.s. = not significant.

examined in both groups. Although children in both groups exhibited similar per cent normal disfluencies ($P = 0.782$), they differed significantly in per cent stuttered disfluencies in speech ($P < 0.001$).

Magnetic resonance imaging data

Among the 56 children who participated, all but one subject's DTI data set (28 controls, 27 stuttering) were acceptable for analyses. Resting state functional MRI data from three controls and seven children who stutter were excluded due to excessive movement; hence 46 (26 controls, 20 stuttering) resting state functional MRI data sets were used for functional connectivity analyses.

Children who stutter have attenuated functional and structural connectivity in the basal ganglia-thalamocortical network, including the putamen and supplementary motor area

Whole brain seed-based functional connectivity comparisons of resting state functional MRI data

Whole-brain group contrast maps showed significant differences between the stuttering and control groups in functional connectivity occurring among regions within the left BGTC loop: when examining brain activity correlation with the left putamen, the control group exhibited significantly higher correlation in the left SMA, left insula, and right posterior superior temporal gyrus relative to the stuttering group (Fig. 1A and Table 2). Children who stutter had greater connectivity with the putamen in the right superior frontal area (Table 2). When examining functional connectivity with left SMA, there were increased correlations in the left posterior-dorsal putamen, left cerebellum, left insula, and right posterior superior temporal gyrus for control subjects relative to children who stutter (Fig. 1B and Table 2).

Pair-wise correlation analyses of regions of interest

We additionally performed pair-wise correlation analyses among several regions of interest within this BGCT network in the left hemisphere (SMA-putamen, SMA-M1, posterior superior temporal gyrus-putamen, M1-putamen). The correlation between SMA and putamen was significantly greater in controls relative to children who stutter [$F(1,39) = 6.15$, $P = 0.018$] (Fig. 1C). There was a significant sex effect for the SMA-putamen correlation [$F(1,39) = 6.732$, $P = 0.013$], but no Group × Sex interaction [$F(1,39) = 0.236$, $P = 0.63$]. There was also a significant effect of age for this correlation [$F(1,39) = 5.712$, $P = 0.022$] (Supplementary Fig. 2A).

Structural connectivity among basal ganglia-cortical areas using probabilistic tractography

The DTI tractography results indicated increased structural connectivity from the left putamen to the left inferior frontal gyrus, middle frontal gyrus, middle temporal gyrus, and insula among others, in controls relative to the stuttering group (Fig. 2C and Table 3). The results also showed that the control group had stronger connections from the left SMA-associated white matter seed to the bilateral precuneus, left cingulate gyrus, and the left putamen, among others (whole brain corrected $P \leqslant 0.033$), compared with the stuttering group (Table 3).

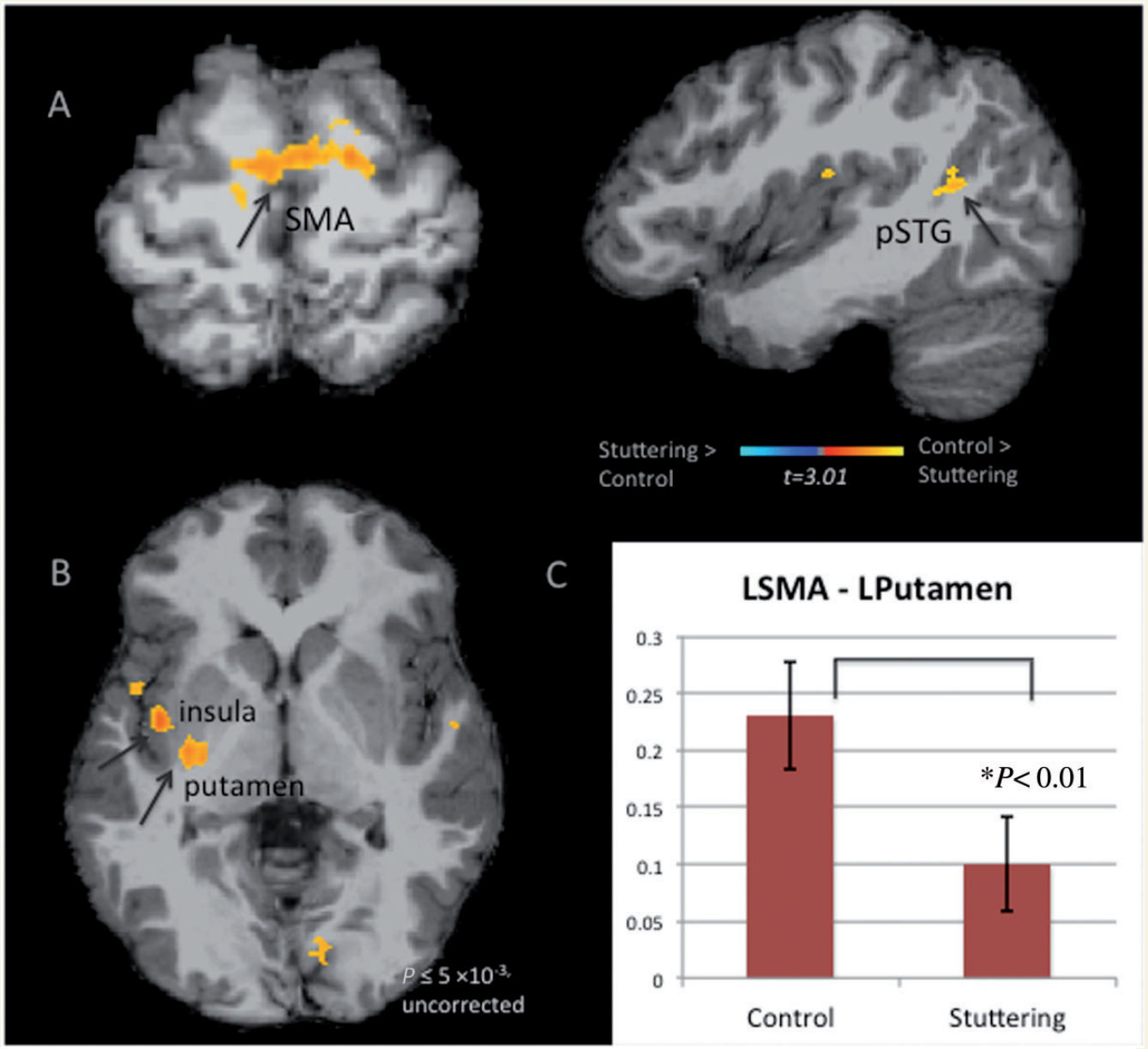

Figure 1 Group differences in functional connectivity based on seeds within the BGTC loop. Warmer colour highlights areas with significantly heightened functional connectivity with a given seed for the controls versus stuttering. Statistical maps are overlaid on a T_1 image of one subject transformed to the MNI 305 template and are thresholded at $P < 0.03$ (corrected). All brains are shown in the neurological convention. (**A**) Functional connectivity maps generated based on the left putamen seed. Here the main differences between the groups were in the SMA and parts of the posterior superior temporal gyrus (pSTG). Namely, controls had significantly higher functional connectivity between the left putamen and the SMA, posterior superior temporal gyrus compared with children who stutter. (**B**) Functional connectivity maps generated with the left SMA seed. There were no significant group differences with the corrected *P*-value; when the cluster threshold was lowered (but still maintaining voxel-wise $P < 0.005$), there was heightened functional connectivity between the left SMA and the left insula, putamen for control children relative to children who stutter. (**C**) When pair-wise correlation coefficients between the left putamen (LPutamen) and left SMA (LSMA) were calculated and compared between the groups, non-stuttering children exhibited significantly higher correlation between the two regions compared to children who stutter, corroborating the whole-brain analyses of group comparisons shown in **A** and **B**.

Table 2 Regions with significantly increased functional connectivity with seeds in the basal ganglia-thalamocortical network (putamen, SMA)

Seed	Region with peak functional connectivity (approximate Brodmann area) (left/right)	Volume (mm^3)	max *t*	*x*	*y*	*z*
L Putamen	***Controls* > *Stuttering***					
	Precuneus (L)/parahippocampal gyrus (18/30) (L)	3162	4.6193	−18	−54	1
	SMA (6)(L)	2118	4.1122	−4	−9	58
	Posterior cingulate (31/18)(L)	1695	4.5165	−1	−70	13
	Precuneus (R)/parahippocampal gyrus (17) (R)	879	4.1147	16	−43	2
	STG (R)	671	4.7606	47	−40	5
	SMA/Cingulate gyrus (6) (L)	592	4.9942	−8	−7	47
	Insula (13)/OP3/rolandic operculum (L)	525	4.0483	−37	−14	13
	Stuttering* > *Controls					
	SFG (8) (R)	825	−4.202	40	29	57
	SFG (R)	512	−4.0731	35	56	10
L SMA	***Controls* > *Stuttering***					
	Putamen/lentiform nucleus (L)	1025	4.442	−23	0	−14
	Cerebellum (Culmen) (VI) (L)	593	3.8968	−29	−52	−23
	pSTG (R)	426	4.419	43	−43	15
	Stuttering* > *Controls					
	Cerebellum (Crus 1) (L)	1665	−4.6237	−42	−69	−34
	Area 4a (paracentral lobule) (R)	1417	−3.9516	9	−32	66

Coordinates are reported in MNI space.
L = left; R = right; STG = superior temporal gyrus; pSTG = posterior superior temporal gyrus; OP3 = Operculum 3; SFG = superior frontal gyrus.

Children who stutter exhibit attenuated functional and structural connectivity within the auditory-motor network

Whole brain seed-based functional connectivity comparisons of resting state functional MRI data

In previous studies examining stuttering speakers, commonly reported results suggested possible deficiencies in connectivity involving the left motor and auditory cortical areas (Lu *et al*., 2009, 2012; Chang *et al*., 2011), and increases in structural volume (Foundas *et al*., 2001) and functional hyperactivity in the right cortical areas (Fox *et al*., 1996; Braun *et al*., 1997; De Nil *et al*., 2000). Given this, we examined network connectivity using bilateral pars opercularis (BA44) and posterior superior temporal gyrus seeds to examine intrinsically correlated brain activity patterns using resting state functional MRI data (Tables 4 and 5). When examining correlated activity with the left pars opercularis seed, both groups showed the expected pattern of correlated activity with this seed in regions including the motor cortex, premotor, and auditory areas (Supplementary Fig. 3). No group differences survived the threshold, although for the left pars opercularis, the controls seemed to have more extensive correlations with the left posterior superior temporal gyrus than in stuttering (Supplementary Fig. 3). When examining functional correlations with the left posterior superior temporal gyrus seed, we found heightened correlations with the cerebellum for stuttering speakers, whereas in controls there were heightened correlations with the left SMA, left inferior frontal gyrus, and bilateral insula relative to children who stutter (Fig. 3A and B and Table 5). Some group differences were also noted when examined with right hemisphere seeds (Table 5).

Pair-wise correlation analyses of regions of interest

We further examined pair-wise correlation coefficients between *a priori* defined pairs of regions within the auditory-motor network using subject-specifically defined regions of interest (LBA44-LpSTG, LBA44-LM1, RBA44-RpSTG, RBA44-RM1). The Fisher Z transformed scores were entered into a two-way ANCOVA with group and sex as between subject factors. The ANCOVA showed no statistically significant overall group effect. However, significant Group × Sex interactions were found in the connectivity between LBA44-LM1 [$F(1,39) = 5.18$, $P = 0.028$], RBA44-RM1 [$F(1,39) = 5.11$, $P = 0.030$], and RBA44-RpSTG [$F(1,39) = 4.50$, $P = 0.040$] (Fig. 3C). When the stuttering and control groups were compared within each sex, group effect did not reach significance in the females. In the male group, stuttering boys exhibited decreased functional connectivity compared to non-stuttering boys in RBA44-RpSTG [$F(1,19) = 4.67$, $P = 0.044$], and approached significance between RBA44-RM1 [$F(1,19) = 3.46$, $P = 0.078$] (Fig. 3C). The group difference approached significance in connectivity between LM1-LBA44 [$F(1,19) = 3.70$, $P = 0.07$]; however, when age was entered as a covariate this group difference was further reduced [$F(1,19) = 0.46$, $P = 0.51$]. There was a significant effect of age for the correlation between LM1-LBA44 [$F(1,19) = 10.83$, $P = 0.004$] (Supplementary Fig. 2B).

Structural connectivity among auditory-motor regions

Group contrasts showed significantly greater structural connectivity between the left pars opercularis seed and left posterior temporal areas via the insula, putamen, and extreme capsule in controls compared with children who stutter (Fig. 2B and Table 6). There were fewer group differences when using the right pars opercularis seed. However, control subjects had greater

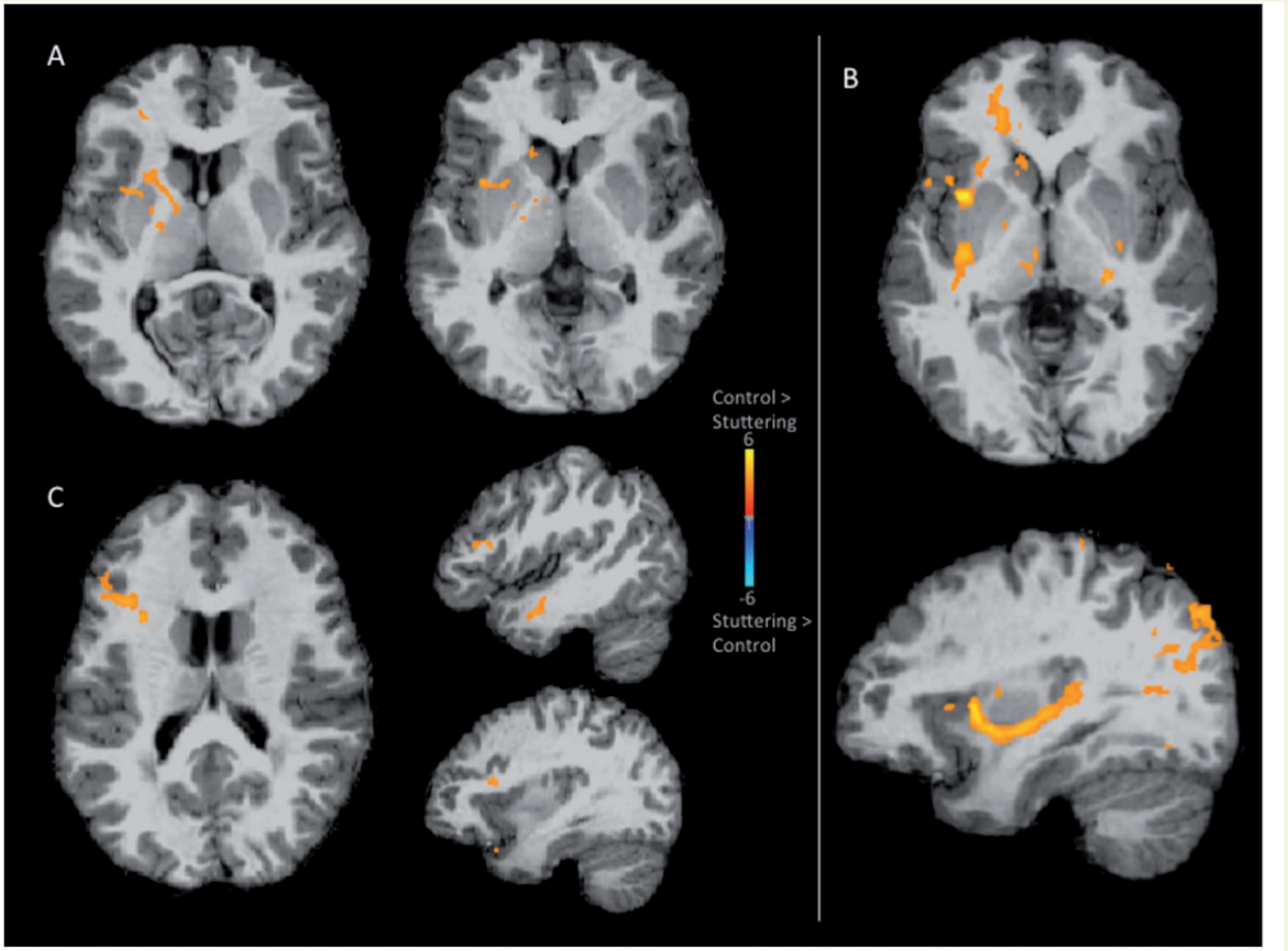

Figure 2 Group differences in white matter probabilistic tractography results. The tracts were thresholded at $P < 0.033$ (corrected; see text for details). Colour highlights areas where control children had significantly greater probability of tracts compared with children who stutter. (**A**) Tractography results based on the left posterior superior temporal gyrus seed. There was significantly stronger connection from this seed to the internal capsule, insula, putamen, caudate, and inferior frontal gyrus in controls relative to the stuttering group. (**B**) Tractography results based on the left pars opercularis (BA44) seed. There was significantly stronger connectivity from this seed to the insula, and reaching the posterior temporal areas through the extreme capsule fibre system in the control group compared to the stuttering group. (**C**) Tractography results based on the left putamen seed. There was significantly stronger connectivity from the left putamen to the inferior frontal region and the middle temporal gyrus areas in control subjects compared with the stuttering group.

connectivity between this seed and subcortical areas such as the putamen, compared to children who stutter (Table 6). The comparison also showed that the controls had greater connectivity from the left posterior superior temporal gyrus to the insula, putamen, internal capsule, among other areas (Fig. 2A and Table 7).

Discussion

Our major new findings are as follows: (i) children who stutter exhibited attenuated functional connectivity among major brain areas within the BGTC loop, including the SMA and putamen. These areas are relevant to potential pathophysiology of stuttering, given that they have been shown to support timing of self-initiated movement (Cunnington *et al*., 1996; Taniwaki *et al*., 2003; Wiese *et al*., 2004; Wu *et al*., 2011), complex sequential motor control (Boecker *et al*., 1998), inhibition of unwanted movements (Marsden and Obeso, 1994), and sensorimotor learning (Doyon *et al*., 2003; Lehéricy *et al*., 2005; Hardwick *et al*., 2013), among other functions. The putamen and SMA may also interact with cortical auditory-motor systems relevant to speech processing (Geiser *et al*., 2012); (ii) boys who stutter, but not girls, exhibited attenuated functional connectivity between ventral premotor/pars opercularis and posterior superior temporal gyrus areas in both hemispheres; and (iii) structural (white matter) connectivity among the putamen and cortical motor and auditory regions is attenuated in the left hemisphere in children who stutter relative to control children, largely corroborating the findings from the functional connectivity results. These results together provide strong evidence supporting significant differences in brain connectivity even at a very young age in children who are relatively close to the onset of stuttering, compared to their non-stuttering

Table 3 Regions with significantly increased structural connectivity with seeds in the BGTC network (putamen, SMA)

Seed	Region with significant tract probability	Cluster size (mm^3)	max *t*	*x*	*y*	*z*
L Putamen	***Controls* > *Stuttering***					
	IFG(44) (L)	483	4.09	−35	18	15
	MTG (L)	255	3.81	−46	−6	−21
	Insula (L)	81	4.39	−28	12	16
	Medial temporal pole	62	3.9	−38	14	−37
	Temporal pole (L)	52	3.68	−35	18	−27
	MTG (21)(L)	38	3.69	−55	1	−27
	Thalamus (L)	36	3.2	−3	−8	12
	ITG (20) (L)	34	3.54	−59	−11	−29
	Stuttering* > *Controls					
	N/A					
L SMA	***Controls* > *Stuttering***					
	Precuneus (L)	792	3.82	−5	−61	41
	Precuneus (R)	328	3.6	20	−44	34
	Precuneus (R)	226	3.73	7	−75	25
	Cingulate gyrus (6)(L)	207	3.75	−6	2	38
	Hypothalamus (R)	197	3.88	8	−1	−15
	Insula (R)	187	3.4	31	−32	17
	Putamen (L)	134	3.68	−21	−8	13
	Precentral gyrus (6)(L)	129	3.8	−27	−11	72
	Cerebellum (Crus1)(R)	117	3.85	38	−72	−36
	Caudate nucleus (R)	103	4.09	13	8	−12
	SMA (L)	97	4.2	−5	1	60
	Caudate (R)	94	4.03	17	6	15
	Thalamus (R)	86	3.75	24	−21	−4
	Postcentral gyrus (R)	74	3.6	26	−33	55
	Cingulate gyrus (24)(L)	62	3.57	−8	−15	37
	IFG/MFG (R)	52	3.44	30	38	9
	Cingulate gyrus (R)	43	3.56	24	−26	34
	Fusiform gyrus (R)	43	3.64	25	5	−47
	Thalamus (L)	41	3.68	1	−15	1
	Stuttering* > *Controls					
	N/A					

IFG = inferior frontal gyrus; ITG = inferior temporal gyrus; L = left; MFG = middle frontal gyrus; MTG = middle temporal gyrus; R = right.

Table 4 Regions with significantly increased functional connectivity with inferior frontal (pars opercularis) seeds

Seed	Region with peak functional connectivity	Volume (mm^3)	max *t*	*x*	*y*	*z*
L pOP	***Controls* > *Stuttering***					
	Stuttering* > *Controls					
	Angular gyrus (39)(R)	542	−4.027	49	−73	32
	MTG (21) (R)	479	−4.311	67	−10	−6
	MFG (R)	420	−3.89	32	15	52
	Precuneus (R)	347	−3.687	12	−67	35
R pOP	***Controls* > *Stuttering***					
	Precentral gyrus (6/4a)(L)	1391	4.5596	−49	−9	36
	Stuttering* > *Controls					
	ITG (37) (R)	1407	−5.3469	55	−49	−9
	ITG (20) (L)	428	−4.3281	−47	−15	−26

ITG = inferior temporal gyrus; L = left; MFG = middle frontal gyrus; MTG = middle temporal gyrus; pOP = pars opercularis; R = right.

Table 5 Regions with significantly increased functional connectivity with auditory (posterior superior temporal gyrus) seeds

Seed	Region with peak functional connectivity	Volume (mm^3)	max *t*	*x*	*y*	*z*
L pSTG	***Controls*** > ***Stuttering***					
	Insula (R)	4713	4.725	40	−14	10
	Insula/IFG (13/44) (L)	1780	4.824	−40	8	3
	SMA (6) (R)	1191	5.0086	5	−1	51
	Cuneus (18) (R)	1002	4.4838	18	−88	22
	Postcentral gyrus (43)/OP4 (L)	520	3.8586	−54	−18	21
	Precentral gyrus (6)(R)	503	4.4498	68	−18	48
	Cuneus (18) (L)	488	3.9704	−9	−94	23
	Precentral gyrus (6)(R)	436	4.612	46	−18	68
	Stuttering > ***Controls***					
	Cerebellum (Crus 1)	830	−4.4565	−26	−65	−33
	ITG (L)	697	−5.0421	−55	−65	−9
	MTG (21) (R)	693	−4.0432	70	−36	−12
	SMG (L)	678	−4.1599	−42	−41	37
	ITG (R)	502	−4.4956	64	−20	−19
	ITG (37)(R)	497	−4.0209	59	−61	−12
	STG (22)(R)	490	−4.3321	69	−57	22
R pSTG	***Controls*** > ***Stuttering***					
	Cuneus (18)(L)	1029	3.6572	−18	−96	8
	SMA (6)(L)	677	3.9728	−9	−23	65
	Stuttering > ***Controls***					
	Cerebellum (Crus 1) (R)	1311	−3.9457	37	−60	−38
	SFG/MFG (R)	1275	−4.5301	30	20	55
	Angular gyrus (39) (R)	552	−4.0097	60	−58	22
	Cerebellum (Crus 1) (L)	497	−3.928	−27	−62	−34

IFG = inferior frontal gyrus; ITG = inferior temporal gyrus; MFG = middle frontal gyrus; MTG = middle temporal gyrus; pSTG = posterior superior temporal gyrus; SFG = superior frontal gyrus; SMG = superior middle gyrus.

peers. In sum, neural networks that support, among other functions, normal timing of self-initiated motor sequences, a skill critical in achieving fluent speech production, seem to be affected in children who stutter. These results are discussed in more detail below.

Children who stutter have attenuated connectivity in the basal ganglia thalamo-cortical network

Functional and structural connectivity between the putamen and SMA captured with resting state functional MRI and DTI tractography, respectively, were significantly lower in children who stutter relative to age-matched peers. The putamen and SMA are part of a network that also includes the premotor cortex and superior temporal gyrus that supports timing of self-paced motor sequences. These networks are more active during self-initiated rather than externally triggered movements (Cunnington *et al.*, 1996; Taniwaki *et al.*, 2003; Wiese *et al.*, 2004). The fact that children who stutter exhibited less connectivity within this network is reconcilable with a well known phenomenon in stuttering speakers: stuttering only occurs during self-paced propositional speech, whereas when instructed to speak in synchrony with external pacing signals like a metronome beat, they can be dramatically fluent (Wingate *et al.*, 2002). A recent study compared brain activity of stuttering and non-stuttering adult speakers during solo, chorus and externally paced reading with functional MRI and found that stuttering adults had decreased activity in the motor regions (SMA, putamen, inferior frontal gyrus and insula) that normalized during the fluency-induced conditions (i.e. chorus and metronome paced), and particularly during metronome timed speech (Toyomura *et al.*, 2011). In addition to normalized activity patterns in motor areas, there were significant increases in auditory cortex activity during the induced fluency conditions in stuttering speakers. These differences were mostly left lateralized, consistent with another study that found left hemisphere differences in the BGTC connectivity in stuttering speakers compared to control subjects (Lu *et al.*, 2010). Hence the current data with children involving the BGTC loop seem to be largely consistent with findings from stuttering adults, indicating that differences in BGTC function may be an important neural signature present in stuttering speakers.

Induced fluency through external pacing, choral reading, and other conditions in people who stutter is similar to findings in patients with Parkinson's disease, where external pacing signals can often assist a patient to initiate movements. In patients with Parkinson's disease, it has been shown that striatal-cortical and striatal-cerebellar connectivities are reduced, whereas cortical-cerebellar connectivity is heightened relative to controls (Wu *et al.*, 2011). The cortical-cerebellar network, which includes the lateral premotor cortex and the cerebellum, has been suggested to be active for patients with Parkinson's disease during externally

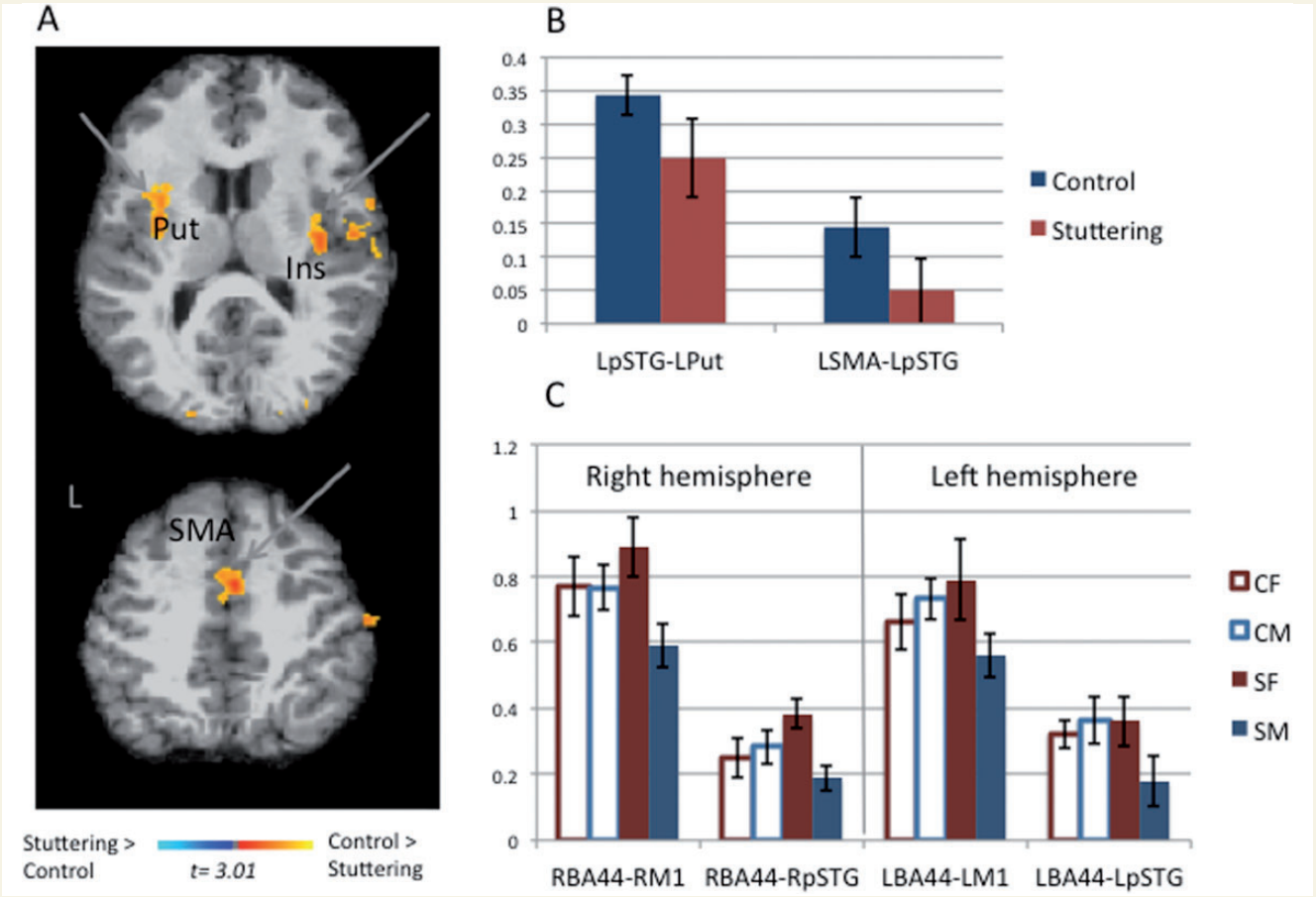

Figure 3 Group differences in functional connectivity based on seeds within the auditory-motor network. Warmer colour indicates areas with significantly heightened functional connectivity with a given seed for the controls versus stuttering. Statistical maps are overlaid on a T_1 image of one subject transformed to the MNI 305 template and are thresholded at $P < 0.03$ (corrected). The brains are shown in the neurological convention. (**A**) Functional connectivity maps generated based on the left posterior superior temporal gyrus seed. Control children had significantly greater functional connectivity with this seed relative to children who stutter in the left putamen (Put), bilateral insula (Ins), and the SMA. (**B**) Pair-wise correlation coefficients showing group differences for correlations between left posterior superior temporal gyrus-left putamen (LPut), left SMA (LSMA)-left posterior superior temporal gyrus (LpSTG). Although clear trends for control children greater than stuttering were seen for both pairs of correlation coefficients, these results did not reach statistical significance. (**C**) Pair-wise correlations among regions within the perisylvian auditory-motor networks (BA44, M1, posterior superior temporal gyrus). Here sex differences within the stuttering group are evident: whereas boys who stutter tend to have the lowest functional connectivity of all groups, girls who stutter tended to be similar or exceed in functional connectivity values relative to all groups. The difference between control children and boys who stutter were significant for RBA44-RM1 and approached significance in RBA44-RpSTG. CF = control female; CM = control male; SF = stuttering female; SM = stuttering male.

guided movements with sensory cues, suggesting that this network may serve as a compensatory mechanism to overcome deficits in the BGTC network. Similarly, the lateral premotor-cerebellar network has also been speculated to allow stuttering speakers to compensate for a weaker cortical-striatal system (Alm, 2004). Indeed, commonly found results in stuttering include hyperactivity in the lateral premotor cortex (Fox *et al*.,1996; Braun *et al*., 1997; Watkins *et al*., 2008; Chang *et al*., 2009) and cerebellum (Fox *et al*., 1996; De Nil *et al*., 2003). The cerebellar activity also correlates with fluent speech in people who stutter (Fox *et al*., 2000), and hyperactivity here often normalizes with therapy but not completely (De Nil *et al*., 2003). It may be possible that during the induced fluency conditions such as paced speech and choral reading, the premotor-cerebellum network overrides the defective BGTC network to instead provide the needed timing cues for speech, by making use of the external sensory (auditory) cues that are given. This may be why, despite findings of both structural and functional network differences in the BGTC network, these 'speech tricks' could result in induced fluency.

Several lines of data have supported a possible abnormality in the BGTC loop in stuttering speakers. Many cases of neurogenic stuttering involve basal ganglia and thalamus lesions (Lundgren *et al*., 2010; Theys *et al*., 2011, 2012), although many neurogenic cases also report a previous history of developmental stuttering (Helm-Estabrooks *et al*., 1986; Mouradian *et al*., 2000). Many (but not all) stuttering speakers benefit from the administration

Table 6 Regions with significantly increased structural connectivity with inferior frontal pars opercularis seeds

Seed	Region with significant tract probability	Cluster size (mm^3)	max *t*	*x*	*y*	*z*
L pOP	***Controls* > *Stuttering***					
	Insula (L)	1302	5.88	−34	6	−2
	Precuneus (L)	1136	4.62	−14	−50	32
	SFG (L)	351	3.96	−20	46	0
	Putamen (L)	250	4.63	−23	−1	14
	Precuneus (R)	247	4.62	26	−46	38
	Red nucleus (L)	231	4.29	−4	−21	−16
	IPL (L)	210	4.56	−30	−81	42
	Postcentral gyrus (R)	180	4.22	17	−50	72
	Insula (L)/pSTG (L)	108	3.75	−29	−38	16
	MTG (L)	68	3.81	−30	−76	20
	Cingulate gyrus (31) (R)	61	4.03	19	−41	32
	Putamen (L)	55	3.84	−24	−6	5
	Thalamus (L)	45	3.63	−16	−11	12
	Caudate nucleus (L)	43	3.86	−17	−8	25
	Thalamus (R)	39	4.09	27	−27	−2
	Thalamus (L)	34	3.98	−9	−28	8
	Stuttering* > *Controls					
	N/A					
R pOP	***Controls* > *Stuttering***					
	SFG (10)(R)	655	4.27	30	62	−11
	Precuneus (L)	273	3.94	−15	−47	34
	Putamen (R)	144	3.73	30	18	3
	SFG (R)	129	3.79	29	50	13
	Putamen (R)	126	3.58	36	−3	7
	Insula (R)	120	3.59	33	−28	18
	Caudate nucleus (R)	76	3.51	19	17	7
	Precuneus (R)	61	3.26	26	−52	24
	Caudate nucleus (R)	52	3.61	22	29	−5
	Fusiform gyrus (R)	50	3.71	41	−65	−8
	Putamen (R)	49	3.49	35	8	−2
	Stuttering* > *Controls					
	N/A					

IPL = inferior parietal lobule; L = left; MTG = middle temporal gyrus; pOP = pars opercularis; R = right; SFG = superior frontal gyrus; STG = superior temporal gyrus.

of dopamine antagonists (e.g. haloperidol, risperidone) (Maguire *et al*., 2000) while pharmacological enhancement of dopamine transmission (e.g. theophylline) often worsens stuttering (Movsessian, 2005). In a small PET study, stuttering speakers were found to have abnormal dopamine metabolism during both stuttering and fluent speech (Wu *et al*., 1997). In another study using functional MRI, stuttering severity was found to be negatively correlated with activity in the basal ganglia, both before and after speech therapy (Giraud *et al*., 2008). All of the above studies have only been conducted with adults who stutter, and have not been tested in children who stutter. Others have conducted modelling work to test hypotheses on the potential effect of dopamine imbalance in stuttering (Civier *et al*., 2011) as well as white matter abnormalities (Civier *et al*., 2013). Using a neurobiologically plausible model of speech production (Guenther *et al*., 2006; Bohland *et al*., 2010), the authors tested the hypothesis that an excess in dopamine would cause overexcitation of the thalamus, in effect disrupting the basal ganglia input to the ventral premotor cortex. According to this model, ventral premotor cortex normally enables selection and execution of the next syllable to be produced. When there is dopamine excess, however, the normal process of selecting the intended syllable while inhibiting all other unwanted syllables is affected, and hence the speaker cannot move on to the next syllable, resulting in a stuttered block or prolongation (Civier *et al*., 2011, 2013). White matter abnormalities similarly may lead to 'transmission errors, and those translate to generation of a weaker contextual signal in the putamen D2 receptor cells'. The result is that selection of the subsequent syllable to be produced is delayed, in turn resulting in stuttering (Civier *et al*., 2013).

In recent functional MRI studies, Lu *et al*. (2010) used structural equation modelling and found that stuttering speakers had stronger connectivity from the putamen to the thalamus, as well as from the thalamus to the temporal and pre-SMA regions, while they exhibited weaker connectivity from the left posterior middle temporal gyrus to the putamen (Lu *et al*., 2010). Together with the present results, these data suggest that stuttering speakers exhibit significant differences compared with control subjects in the way that the basal ganglia structures interact with the cortical areas that support speech motor planning and execution.

Table 7 Regions with significantly increased structural connectivity with auditory (posterior superior temporal gyrus) seeds

Seed	Region with significant tract probability	Cluster size (mm^3)	max *t*	*x*	*y*	*z*
L pSTG	***Controls* > *Stuttering***					
	Insula/extreme capsule (L)	1123	4.11	−34	1	−5
	Precuneus (R)	277	3.5	23	−52	43
	Cingulate gyrus (32) (L)	209	3.68	−16	11	41
	Putamen/internal capsule (L)	191	3.64	−20	−11	13
	Medial temporal pole (R)	115	3.59	34	14	−37
	Putamen (L)	114	3.65	−22	−5	8
	MFG (L)	109	3.4	−24	21	28
	Cuneus (R)	98	3.42	29	−72	17
	Precuneus (L)	83	3.32	−19	−64	46
	Cerebellum (VIII)(R)	82	3.46	34	−50	−44
	Precuneus (R)	81	3.44	14	−62	34
	Cerebellum (X)(R)	74	3.3	25	−38	−40
	MFG (L)	70	3.22	−27	39	4
	Precuneus (L)	57	3.38	−31	−85	37
	Red nucleus (L)	54	3.54	−4	−16	−9
	Putamen/lentiform nucleus (R)	44	3.58	30	−11	−6
	Caudate (L)	42	3.42	−12	17	1
	STG (L)	35	3.41	−60	−41	21
	Cerebellar tonsil (Crus 2)	32	3.3	−46	−55	−47
	Stuttering* > *Controls					
	N/A					
R pSTG	***Controls* > *Stuttering***					
	IPL/SMG (R)	317	4.85	54	−25	30
		181	3.88	54	−33	39
	Anterior insula (R)	105	3.49	42	14	−13
	IFG (R)	105	3.4	32	38	5
	SFG (R)	70	3.42	23	54	−9
	Insula (R)	64	3.33	33	−28	17
	MTG (R)	57	3.38	53	−46	−3
	Postcentral gyrus (R)	33	3.39	55	−16	30
	Putamen/Internal capsule (R)	33	3.28	20	19	−2
	Stuttering* > *Controls					
	STG (R)	40	−3.53	67	−23	−2

IFG = inferior frontal gyrus; IPL = inferior parietal lobule; MFG = middle frontal gyrus; pSTG = posterior superior temporal gyrus; SFG = superior frontal gyrus; SMG = superior middle gyrus.

In behavioural studies that examined motor sequence learning, stuttering speakers were found significantly less accurate and slower in these tasks, and in particular, did not seem to develop automaticity of movement with practice (Smits Bandstra and De Nil, 2009). In preschool-age children who stutter, interarticulator motions during accurate and fluent productions of the non-words showed higher variability in oral motor coordination indices, indicating that children who stutter lagged their typically developing peers in maturation of speech motor control processes (Smith *et al*., 2012). Subtle deficits in the ability to shift from an effortful, sensory feedback-based motor execution to a more automatic feedforward-based processing have been proposed to be what underlies stuttering (Max *et al*., 2004). Although more detail needs to be brought about, there is mounting evidence pointing to potential deficiencies in the development of efficient speech motor control in children who stutter. The current neuroimaging data, showing differences in the BGTC loop previously shown to support automatic, well-learned, self-paced movement, seems to corroborate these behavioural results that have been shown in both children and adults who stutter. Further detailed studies examining the connectivity among BGTC loop regions is warranted and may lead us into a clearer understanding about the nature and neural bases of motor planning, sequencing, and execution processes in people who stutter.

Differences in cortical networks supporting auditory-motor integration for speech production

In past studies examining stuttering adults, brain activity patterns during various speech production tasks found a lack of auditory cortex activity and overactivity in the motor regions. Relative to the non-stuttering control group, stuttering speakers exhibited heightened activity in the right hemisphere in motor regions (Fox *et al*., 1996; Braun *et al*., 1997; Chang *et al*., 2009). The

apparent discrepancy in the level of activity between the motor and auditory areas in stuttering speakers (Fox *et al*., 1996; Braun *et al*., 1997), and abnormal anatomy focused in these regions, particularly in the left hemisphere (Sommer *et al*., 2002; Chang *et al*., 2008, 2011; Cykowski *et al*., 2010), may indicate inefficient connections among these regions. In this context, right-sided overactivity could be explained as a compensatory reaction to the left-sided deficit.

Consistent with previous studies based on adults who stutter, we found attenuated connectivity among cortical auditory-motor regions in children who stutter relative to control children. In particular there was decreased connectivity between the posterior superior temporal gyrus and the insula, SMA, and the inferior frontal gyrus focused in the left hemisphere. Whereas both boys and girls who stutter exhibited similarly decreased connectivity measures within the BGTC network relative to control children, in the auditory-motor network, pair-wise correlations between regions accentuated heightened differences only within the male group of children who stutter. In addition, group differences approached significance for the connectivity between left motor (M1) and left pars opercularis (BA44) regions in boys (but not girls) who stutter compared with boys who do not stutter. Correlated activity at rest between these two motor regions seemed to decrease with age for both groups. These age effects, however, may have been driven at least in part by some exclusion of data sets from our youngest stuttering boys because of movement artefacts. Hence, these results need to be confirmed with larger samples in the future.

Likewise, because we only had a few stuttering girls in this sample, sex differences within the stuttering group should be interpreted with caution and should be confirmed with larger samples in future studies. However these preliminary results provide some interesting issues to consider for future studies. The skewed sex ratio in persistent stuttering is well established: many more males stutter than females, although close to onset the sex ratio is more similar (Yairi and Ambrose, 1992). This indicates a much higher rate of spontaneous recovery from stuttering in girls who stutter. It is possible that our sample of girls who stutter may have included those who may recover during future development, and hence may have exhibited more normalized neural development, which may later coincide with recovery from stuttering. The left motor to left pars opercularis connectivity decreases found in boys and not girls who stutter may indicate that intact connectivity in this region may correlate with eventual recovery from stuttering, which is more common in girls. These speculations can be examined in more detail in future studies as we recruit more boys and girls who stutter, and collect multiple brain data each year from the same children, which will allow longitudinal analyses of their brain developmental trajectories and behavioural speech measures.

Although we were able to replicate findings of primarily left-sided auditory-motor connectivity decreases in children who stutter, there were some differences from what have been reported in previous studies. Using the left posterior superior temporal gyrus seed (but not with the pars opercularis seeds) we were able to find functional connectivity differences between stuttering and control groups of children. In white matter tractography, using the left pars opercularis seed derived group differences in the tract that interconnected with the posterior temporal region through a ventrally located tract through the extreme capsule fibre system, not through the dorsal superior longitudinal fasciculus that was commonly found in previous investigations in stuttering speakers (Sommer *et al*., 2002; Chang *et al*., 2008, 2011; Cykowski *et al*., 2010). According to other DTI studies it was reported that the more rostrally located inferior frontal area, pars triangularis, connects with the posterior superior temporal gyrus through the extreme capsule fibre system, whereas the more dorsally located pars opercularis connects to the inferior parietal lobule/posterior superior temporal gyrus via the superior longitudinal fasciculus (Frey *et al*., 2008; Kelly *et al*., 2010). It is possible that, because of normally occurring structural variability within the inferior frontal gyrus regions that some of our pars opercularis regions of interest included parts of pars triangularis, which may have driven the group differences found in the extreme capsule. Work is underway (Tourville and Guenther, 2012) to help provide a more detailed and reliable distinction between the pars opercularis and pars triangularis areas, and application of these detailed maps to our data analyses may elucidate this issue in future studies.

Although there are some disagreements on the specific tracts involved, a consistent finding that seems to emerge in stuttering speakers is a decrease relative to controls in long-range white matter tracts interconnecting frontal motor and posterior auditory areas in the left hemisphere. Insufficient white matter integrity between these regions may lead to subtle inefficiencies in one's ability to match the auditory target associated with one's own motor execution (articulation) to actual auditory feedback. If a mismatch occurs between the intended (predicted) auditory target of the speech produced and the actual auditory feedback, the auditory cortex sends corrective signals to the motor system to modify the motor programme for subsequent articulations (Guenther, 1994; Hickok *et al*., 2011). During such perturbations and resulting auditory feedback guided speech compensation, it has been shown that the auditory cortex heightens activity (Houde *et al*., 2002). Recently it was shown that this 'speech perturbation related enhancement' in the posterior superior temporal gyrus, along with premotor cortex activity, correlated significantly with the amount of behavioural motor compensation to the auditory perturbation (Bouchard *et al*., 2013). According to the authors, speech perturbation related enhancement is a 'hallmark of auditory influence on motor output' and it underlies the speaker's ability to monitor one's own speech and for the online modification and control of speech production (Bouchard *et al*., 2013). Such tight connectivity between the auditory and motor systems allows auditory feedback to be used to make adjustments and fine-tune subsequent speech movements that are necessary for transitions between the end of an utterance and the beginning of the next utterance (Cai *et al*., 2012). As Cai *et al*. (2012) argue, if there are deficits in auditory-to-motor interactions that normally enables online motor correction, this may lead to 'improper transitions between syllables, leading to disfluencies'. In the present data from stuttering children, attenuated functional and structural connectivity in the left cortico-cortical auditory-motor network is especially evident in boys who stutter and less so in girls who stutter. Aberrant network connectivity here may

exacerbate stuttering and may correlate with persistent stuttering, whereas normalized patterns in this network achieved with development may be correlated with recovery from stuttering. These questions will need to be examined in detail with future longitudinal studies.

Interactions between the basal ganglia-thalamocortical 'motor' circuit and the auditory-motor cortico-cortical networks

Behavioural data showing reduced ability to achieve effortless, automatic motor performance (Smits-Bandstra and De Nil, 2009; Smith *et al*., 2012), attenuated motor compensation when given perturbed sensory feedback (Cai *et al*., 2012), and the accruing functional and structural connectivity neuroimaging evidence reviewed above all point to potential deficiencies in the BGTC networks. Given the addition of the current data from children who stutter, these potential deficits in BGTC networks seem to be present starting in childhood. If adequate connectivity within the BGTC circuit is not well developed, timing of motor sequences could be disrupted, resulting in a disruption in matching between sensory targets and motor planning/execution. With development, such discrepancies in the auditory-motor connectivity may become exacerbated, associated with increased effort and habituated compensatory responses to stuttered speech. These behavioural compensations may further drive structural and functional neuroplastic changes that have been consistently observed in stuttering adults, such as discrepant activity patterns among the left hemisphere motor and auditory areas, heightened motor area activity in general, and increases in right hemisphere volume and activity patterns during speech tasks.

Methodological considerations and future directions

In resting state functional MRI, spontaneous, synchronized fluctuations in the blood oxygen level-dependent signal are analysed as reflecting tightly coordinated and functionally related neural networks. Because these are spontaneous fluctuations that are not induced by any task, the functional brain data are less affected by effort, experience, or strategy, factors that complicate the interpretation of stimulus-based functional MRI data (Casey *et al*., 2005). This makes resting state functional MRI a good method to examine the neuronal networks in both normally and abnormally developing children (Uddin and Menon, 2010). Resting state functional MRI is also useful when applied to examining young children because of its relatively short length (7 min), without the need to ensure task cooperation during scanning. This technique can also be paired with task-based functional MRI that examines performance on speech planning and execution in future studies of stuttering children. These studies are currently being planned for our older participants (aged 7 and up).

For both DTI and resting state functional MRI in this study, our analyses have been hypothesis-driven even in our 'whole-brain' analysis. The functional and structural connectivity maps were derived based on *a priori*-defined seeds—and thus have been limited to examining neural networks that were found to differ in previous studies, mostly based on adults who stutter. Because of neuroplastic changes occurring throughout development, it is possible that children who stutter may exhibit other areas that are different from age-matched peers. Independent component analysis and Graph theory-based analyses allow examination of neural networks not limited to *a priori* circumscribed areas of interest and may be useful to implement in future studies. In particular, Graph theory methods have been shown to be particularly useful in the examination of developing brain networks (Power *et al*., 2010) and developmental disorders. These analyses allow comparisons of long-range versus short-range connections, hierarchical organization and inter-regional interaction of functionally connected regions, which can be tracked across development. We will be pursuing these analyses with larger samples in future studies. Likewise, in our DTI data analyses, methods such as tract-based spatial statistics (Smith *et al*., 2006) will allow examination of whole-brain based differences between groups in the development of white matter tracts.

Another important area that needs to be explored is sex differences in the brain trajectories in stuttering. This study provided some preliminary glimpses into the differences between stuttering boys and girls, but this will need to be examined in the context of eventual persistence versus recovery from stuttering. Several neuroimaging studies have also noted differences between the sexes in stuttering adults (Ingham *et al*., 2004; Chang *et al*., 2009). These studies will potentially provide information on specific neural modification for natural recovery from stuttering, and whether these modifications are sex-specific. These may lead to more focused and specific individualized treatment in the future.

Conclusion

This study reports first evidence of brain functional and structural connectivity differences in children who stutter, involving neural networks that support self-initiated timing of speech movement, and integration of auditory feedback to speech motor control processes. There is strong evidence of structural and functional connectivity decreases in stuttering children in the BGTC and the auditory-motor cortical loops, primarily in the left hemisphere. The presence of these differences in children who stutter as a group, and the preliminary observation that girls who stutter (who are more likely to recover than boys who stutter in future years) had higher connectivity in the auditory-motor regions, suggest that these networks could undergo dynamic changes during development that may underlie natural recovery from stuttering. Given the present findings on connectivity differences in neural networks that are associated with self-initiated movement and internal generation of rhythm that may help guide timing of speech utterances, future studies may test the effects of incorporating rhythm (Zatorre *et al*., 2007) and synchronized speech (Davidow *et al*., 2011) in speech therapy. Such interventions can be tested for their potential effects on normalizing brain structure and functional connectivity that underlies recovery from stuttering.

Acknowledgements

The authors wish to thank all the children and parents who have participated in this study. We also thank Kristin Hicks for her assistance in participant recruitment, behavioural testing, and help with MRI data collection, Margaret Semrud-Clikeman for assistance with neuropsychology assessments, Scarlett Doyle for her assistance in MRI data acquisition, and Ashley Larva and Jennifer Kudsin for their assistance in speech data analyses.

Funding

This study was supported by Award Number #R01DC011277 (PI: Chang) from the National Institute on Deafness and other Communication Disorders (NIDCD). The content is solely the responsibility of the authors and does not necessarily represent the official views of the NIDCD or the National Institutes of Health.

Supplementary material

Supplementary material is available at *Brain* online.

References

Alm PA. Stuttering and the basal ganglia circuits: a critical review of possible relations. J Commun Disord 2004; 37: 325–70.

Association APT. Purdue Pegboard Test. APTA Guide to Physical Therapist Practice 2010; 1: 41358.

Beal DS, Gracco V, Lafaille S, De Nil L. Voxel-based morphometry of auditory and speech-related cortex in stutterers. Neuroreport 2007; 18: 1257.

Beal DS, Gracco VL, Brettschneider J, Kroll RM, De Nil LF. A voxel-based morphometry (VBM) analysis of regional grey and white matter volume abnormalities within the speech production network of children who stutter. Cortex 2012; 1–11.

Behrens T, Berg H, Jbabdi S, Rushworth M, Woolrich M. Probabilistic diffusion tractography with multiple fibre orientations: what can we gain? Neuroimage 2007; 34: 144–55.

Biswal B, Zerrin Yetkin F, Haughton VM, Hyde JS. Functional connectivity in the motor cortex of resting human brain using echo-planar mri. Magn Reson Med 1995; 34: 537–41.

Bloodstein O. A handbook of stuttering. San Diego: Singular Publishing Group, Inc; 1995.

Boecker H, Dagher A, Ceballos-Baumann AO, Passingham RE, Samuel M, Friston KJ, et al. Role of the human rostral supplementary motor area and the basal ganglia in motor sequence control: investigations with H2 15O PET. J Neurophysiol 1998; 79: 1070–80.

Bohland JW, Bullock D, Guenther FH. Neural representations and mechanisms for the performance of simple speech sequences. J Cogn Neurosci 2010; 22: 1504–29.

Bouchard KE, Mesgarani N, Johnson K, Chang EF. Functional organization of human sensorimotor cortex for speech articulation. Nature 2013; 495: 327–32.

Braun A, Varga M, Stager S, Schulz G, Selbie S, Maisog J, et al. Altered patterns of cerebral activity during speech and language production in developmental stuttering. An H2(15)O positron emission tomography study. Brain 1997; 120 (Pt 5): 761–84.

Cai S, Beal DS, Ghosh SS, Tiede MK, Guenther FH, Perkell JS. Weak responses to auditory feedback perturbation during articulation in persons who stutter: evidence for abnormal auditory-motor transformation. PLoS One 2012; 7: e41830.

Casey B, Galvan A, Hare T. Changes in cerebral functional organization during cognitive development. Curr Opin Neurobiol 2005; 15: 239–44.

Chang S, Erickson K, Ambrose N, Hasegawa-Johnson M, Ludlow C. Brain anatomy differences in childhood stuttering. Neuroimage 2008; 39: 1333–44.

Chang S, Horwitz B, Ostuni J, Reynolds R, Ludlow CL. Evidence of left inferior frontal-premotor structural and functional connectivity deficits in adults who stutter. Cereb Cortex 2011; 21: 2507–18.

Chang S, Kenney MK, Loucks TMJ, Ludlow CL. Brain activation abnormalities during speech and non-speech in stuttering speakers. Neuroimage 2009; 46: 201–12.

Civier O, Bullock D, Max L, Guenther FH. Dopamine excess may delay selection of syllabic motor programs: a Modeling study of stuttering. Proceedings of the 17th International Congress of Phonetic Sciences, Hong King, China. 2011. p. 504–7.

Civier O, Bullock D, Max L, Guenther FH. Computational modeling of stuttering caused by impairments in a basal ganglia thalamo-cortical circuit involved in syllable selection and initiation. Brain Lang 2013; 126: 263–78.

Cox R. AFNI: software for analysis and visualization of functional magnetic resonance neuroimages. Comput Biomed Res 1996; 29: 162–73.

Cunnington R, Bradshaw J, Iansek R. The role of the supplementary motor area in the control of voluntary movement. Hum Mov Sci 1996; 15: 627–47.

Cykowski M, Kochunov P, Ingham R, Ingham J, Mangin J, Riviere D, et al. Perisylvian sulcal morphology and cerebral asymmetry patterns in adults who stutter. Cereb Cortex 2008; 18: 571–83.

Cykowski MD, Fox PT, Ingham RJ, Ingham JC, Robin DA. A study of the reproducibility and etiology of diffusion anisotropy differences in developmental stuttering: a potential role for impaired myelination. Neuroimage 2010; 52: 1495–504.

Davidow JH, Bothe AKA, Ye JJ. Systematic studies of modified vocalization: speech production changes during a variation of metronomic speech in persons who do and do not stutter. J Fluency Disord 2011; 36: 93–109.

De Nil L, Kroll R, Kapur S, Houle S. A positron emission tomography study of silent and oral single word reading in stuttering and nonstuttering adults. J Speech Lang Hear Res 2000; 43: 1038–53.

De Nil L, Kroll R, Lafaille S, Houle S. A positron emission tomography study of short- and long-term treatment effects on functional brain activation in adults who stutter. J Fluency Disord 2003; 28: 357–80.

Doyon J, Penhune V, Ungerleider LG. Distinct contribution of the cortico-striatal and cortico-cerebellar systems to motor skill learning. Neuropsychologia 2003; 41: 252–62.

Fischl B, Salat DH, Busa E, Albert M, Dieterich M, Haselgrove C, et al. Whole brain segmentation—automated Labeling of Neuroanatomical structures in the human brain. Neuron 2002; 33: 341–55.

Foundas A, Corey D, Angeles V, Bollich A, Crabtree-Hartman E, Heilman K. Atypical cerebral laterality in adults with persistent developmental stuttering. Neurology 2003; 61: 1378–85.

Foundas AL, Bollich AM, Corey DM, Hurley M, Heilman KM. Anomalous anatomy of speech-language areas in adults with persistent developmental stuttering. Neurology 2001; 57: 207–15.

Fox M, Snyder A, Vincent J, Corbetta M, Van Essen D, Raichle M. The human brain is intrinsically organized into dynamic, anticorrelated functional networks. Proc Natl Acad Sci USA 2005; 102: 9673–8.

Fox P, Ingham R, Ingham J, Hirsch T, Downs J, Martin C, et al. A PET study of the neural systems of stuttering. Nature 1996; 382: 158–61.

Fox PT, Ingham RJ, Ingham JC, Zamarripa F, Xiong JH, Lancaster JL. Brain correlates of stuttering and syllable production. A PET performance-correlation analysis. Brain 2000; 123 (Pt. 10): 1985–2004.

Frey S, Campbell JSW, Pike GB, Petrides M. Dissociating the human language pathways with high angular resolution diffusion fiber tractography. J Neurosci 2008; 28: 11435–44.

Geiser E, Notter M, Gabrieli JDE. A corticostriatal neural system enhances auditory perception through temporal context processing. J Neurosci 2012; 32: 6177–182.

Ghosh SS, Kakunoori S, Augustinack J, Nieto-Castanon A, Kovelman I, Gaab N, et al. Evaluating the validity of volume-based and surface-based brain image registration for developmental cognitive neuroscience studies in children 4 to 11 years of age. Neuroimage 2010; 53: 85–93.

Giraud A, Neumann K, Bachoud-Levi A, Gudenberg von A, Euler H, Lanfermann H, et al. Severity of dysfluency correlates with basal ganglia activity in persistent developmental stuttering. Brain Lang 2008; 104: 190–9.

Greicius MD, Supekar K, Menon V, Dougherty RF. Resting-state functional connectivity reflects structural connectivity in the default mode network. Cereb Cortex 2009; 19: 72–8.

Greicius MD. Functional connectivity in the resting brain: a network analysis of the default mode hypothesis. Proc Natl Acad Sci USA 2002; 100: 253–58.

Guenther F, Ghosh S, Tourville J. Neural modeling and imaging of the cortical interactions underlying syllable production. Brain Lang 2006; 96: 280–301.

Guenther F. A neural network model of speech acquisition and motor equivalent speech production. Biol Cybern 1994; 72: 43–53.

Gusnard DA, Raichle ME, Raichle ME. Searching for a baseline: functional imaging and the resting human brain. Nat Rev Neurosci 2001; 2: 685–94.

Hampson M, Peterson B, Skudlarski P, Gatenby J, Gore J. Detection of functional connectivity using temporal correlations in MR images. Hum Brain Mapp 2002; 15: 247–62.

Hardwick RM, Rottschy C, Miall RC, Eickhoff SB. A quantitative meta-analysis and review of motor learning in the human brain. Neuroimage 2013; 67: 283–97.

Helm-Estabrooks N, Yeo R, Geschwind N, Freedman M, Weinstein C. Stuttering: disappearance and reappearance with acquired brain lesions. Neurology 1986; 36: 1109–12.

Hickok G, Houde J, Rong F. Sensorimotor Integration in Speech Processing: Computational Basis and Neural Organization. Neuron 2011; 69: 407–22.

Hollingshead AB. Four-factor index of social status. Unpublished manuscript. New Haven, CT: Yale University; 1975.

Houde JF, Nagarajan S, Sekihara K, Merzenich M. Modulation of the auditory cortex during speech: an MEG study. J Cogn Neurosci 2002; 14: 1125–38.

Ingham R, Fox P, Ingham J, Xiong J, Zamarripa F, Hardies L, et al. Brain correlates of stuttering and syllable production: gender comparison and replication. J Speech Lang Hear Res 2004; 47: 321–24.

Jancke L, Hanggi J, Steinmetz H. Morphological brain differences between adult stutterers and non-stutterers. BMC Neurol 2004; 4: 23.

Johansen-Berg H, Behrens T. Just pretty pictures? What diffusion tractography can add in clinical neuroscience. Curr Opin Neurol 2006; 19: 379–85.

Kelly C, Uddin LQ, Shehzad Z, Margulies DS, Castellanos FX, Milham MP, et al. Broca's region: linking human brain functional connectivity data and non-human primate tracing anatomy studies. Eur J Neurosci 2010; 32: 383–98.

Lehéricy S, Benali H, Van De Moortele PF, Pélégrini-Issac M, Waechter T, Ugurbil K, et al. Distinct basal ganglia territories are engaged in early and advanced motor sequence learning. Proc Natl Acad Sci USA 2005; 102: 12566–71.

Lu C, Chen C, Peng D, You W, Zhang X, Ding G, et al. Neural anomaly and reorganization in speakers who stutter: a short-term intervention study. Neurology 2012; 79: 625–32.

Lu C, Ning N, Peng D, Ding G, Li K, Yang Y, et al. The role of large-scale neural interactions for developmental stuttering. NSC 2009; 161: 1008–26.

Lu C, Peng D, Chen C, Ning N, Ding G, Li K, et al. Altered effective connectivity and anomalous anatomy in the basal ganglia-thalamocortical circuit of stuttering speakers. Cortex 2010; 46: 49–67.

Lundgren K, Helm-Estabrooks N, Klein R. Stuttering following acquired brain damage: a review of the literature. J Neurolinguistics 2010; 23: 447–54.

Maguire GA, Riley GD, Franklin DL, Gottschalk LA. Risperidone for the Treatment of Stuttering [Internet]. J Clin Psychopharmacol 2000; 20: 479.

Marsden CD, Obeso JA. The functions of the basal ganglia and the paradox of stereotaxic surgery in Parkinson's disease. Brain 1994; 117: 877–97.

Max L, Guenther F, Gracco V, Ghosh S, Wallace M. Unstable or insufficiently activated internal models and feedback-biased motor control as sources of dysfluency: a theoretical model of stuttering. Contemp Issues Commun Sci Disord 2004; 31: 105–22.

Mouradian M, Paslawski T, Shuaib A. Return of stuttering after stroke. Brain Lang 2000; 73: 120–3.

Movsessian P. Neuropharmacology of theophylline induced stuttering: the role of dopamine, adenosine and GABA. Med Hypotheses 2005; 64: 290–7.

Oldfield R. The assessment and analysis of handedness: the Edinburgh inventory. Neuropsychologia 1971; 9: 97–113.

Power JD, Fair DA, Schlaggar BL, Petersen SE. The development of human functional brain networks. Neuron 2010; 67: 14.

Sala-Llonch R, Peña-Gómez C, Arenaza-Urquijo EM, Vidal-Piñeiro D, Bargalló N, Junqué C, et al. Brain connectivity during resting state and subsequent working memory task predicts behavioural performance. Cortex 2012; 48: 1187–96.

Smith A, Goffman L, Sasisekaran J, Weber-Fox C. Language and motor abilities of preschool children who stutter: evidence from behavioral and kinematic indices of nonword repetition performance. J Fluency Disord 2012; 37: 344–58.

Smith S, Jenkinson M, Johansen-Berg H, Rueckert D, Nichols T, Mackay C, et al. Tract-based spatial statistics: voxelwise analysis of multi-subject diffusion data. NeuroImage 2006; 31: 1487–505.

Smith SM, Jenkinson M, Woolrich MW, Beckmann CF, Behrens TE, Johansen-Berg H, et al. Advances in functional and structural MR image analysis and implementation as FSL. [Internet]. Neuroimage 2004; 23(Suppl 1): S208–S219.

Smits Bandstra S, De Nil L. Speech skill learning of persons who stutter and fluent speakers under single and dual task conditions. Clin Linguist Phon 2009; 23: 38–57.

Sommer M, Koch MA, Paulus W, Weiller C, Büchel C. Disconnection of speech-relevant brain areas in persistent developmental stuttering. Lancet 2002; 360: 380–3.

Taniwaki T, Okayama A, Yoshiura T, Nakamura Y, Goto Y, Kira J-I, et al. Reappraisal of the motor role of Basal Ganglia: a functional magnetic resonance image study [Internet]. J Neurosci 2003; 23: 3432–8.

Theys C, De Nil L, Thijs V, van Wieringen A, Sunaert S. A crucial role for the cortico-striato-cortical loop in the pathogenesis of stroke-related neurogenic stuttering. Hum Brain Mapp 2013; 34: 2103–12.

Theys C, van Wieringen A, Sunaert S, Thijs V, De Nil LF. A one year prospective study of neurogenic stuttering following stroke: incidence and co-occurring disorders. J Commun Disord 2011; 44: 678–87.

Tourville J, Guenther F. Automatic cortical labeling system for neuroimaging studies of normal and disordered speech. Soc Neurosci 2012; 1–1.

Toyomura A, Fujii T, Kuriki S. Effect of external auditory pacing on the neural activity of stuttering speakers. Neuroimage 2011; 57: 1507–16.

Uddin LQ, Menon V. Typical and atypical development of functional human brain networks: insights from resting-state fMRI. Front Syst Neurosci 2010; 4: 1–12.

Ward BD. Simultaneous inference for fMRI data. Unpublished AFNI Alphasim Documentation, Medical College of Wisconsin 2000.

Watkins KE, Smith SM, Davis S, Howell P. Structural and functional abnormalities of the motor system in developmental stuttering. Brain 2008; 131: 50–9.

Wiese H, Stude P, Nebel K, De Greiff A, Forsting M, Diener H, et al. Movement preparation in self-initiated versus externally triggered movements: an event-related fMRI-study [Internet]. Neurosci Lett 2004; 371: 220–5.

Wingate ME, Howell AP, Reviewer. Foundations of Stuttering. J Acoust Soc Am 2002; 112: 1229–31.

Wu JC, Maguire G, Riley G, Lee A, Keator D, Tang C, et al. Increased dopamine activity associated with stuttering [Internet]. Neuroreport 1997; 8: 767–70.

Wu JCJ, Maguire GG, Riley GG, Fallon JJ, LaCasse LL, Chin SS, et al. A positron emission tomography [18F]deoxyglucose study of developmental stuttering. [Internet]. Neuroreport 1995; 6: 501–5.

Wu T, Wang L, Hallett M, Chen Y, Li K, Chan P. Effective connectivity of brain networks during self-initiated movement in Parkinson's disease. Neuroimage 2011; 55: 204–15.

Xuan Y, Meng C, Yang Y, Zhu C, Wang L, Yan Q, et al. Resting-state brain activity in adult males who stutter. PLoS One 2012; 7: e30570.

Yairi EE, Ambrose NN. Onset of stuttering in preschool children: selected factors. J Speech Hear Res 1992; 35: 782–88.

Yeo BT, Krienen FM, Sepulcre J, Sabuncu MR, Lashkari D, Hollinshead M, et al. The organization of the human cerebral cortex estimated by intrinsic functional connectivity. J Neurophysiol 2011; 106: 1125–65.

Zatorre R, Chen J, Penhune V. When the brain plays music: auditory-motor interactions in music perception and production. Nat Rev Neurosci 2007; 8: 547–58.

Zhu DC, Majumdar S, Korolev IO, Berger KL, Bozoki AC. Alzheimer's disease and amnestic mild cognitive impairment weaken connections within the default-mode network: a multi-modal imaging study. J Alzheimers Dis 2013; 34: 969–84.